RESEARCH ARTICLE OPEN ACCESS

Effect of Ambient Temperature and Composition on Liquid Droplet Combustion

Shah Shahood Alam
Pollution and Combustion Engineering Lab. Dept. of Mechanical Engineering. Aligarh Muslim University, Aligarh, U.P. India.

ABSTRACT
An unsteady, spherically symmetric, single component, diffusion controlled gas phase droplet combustion model was developed assuming infinite kinetics and no radiation effects. Finite difference technique was used to solve time dependent equations of energy and species. Adiabatic flame temperature which is important for calculating thermodynamic properties was calculated by employing a detailed method. Effects of ambient temperature and composition on important combustion parameters like adiabatic flame temperature, droplet mass burning rate, burning constant and droplet lifetime were obtained. Results indicated that flame temperature, burning constant and mass burning rate increased with an increase in ambient temperature while the droplet life time decreased. The present gas phase code was used in conjunction with the Olikara and Borman code for obtaining concentration of important species. Emission results showed that for a 100 μm n-heptane droplet burning in standard atmosphere, an increase in ambient temperature led to an increase in NO and CO concentrations and a decrease in CO_2 and H_2O concentrations. Extinction diameter for a 3000 μm n-heptane droplet burning in oxygen-helium environment was determined. Also, effects of ambient temperature and composition were obtained on droplet lifetime and mass burning rate as a function of initial droplet diameter. The present gas phase model is simple but realistic and can be incorporated in spray combustion codes.

Keywords: Droplet combustion model, numerical technique, simplified approach, combustion and emission characteristics, extinction diameter, spray combustion application.

I. Introduction

In many engineering applications like diesel engines, gas turbines, industrial boilers and furnaces and liquid rockets, liquid fuel is often atomised into liquid fragments (droplets) so that the total surface area of droplets is much greater than that of the original liquid mass in order to facilitate mixing and overall burning.This act of fragmentation is called spraying. The spray of liquid hydrocarbon fuel is then mixed with the oxidiser and burned in the combustion chamber of various devices.

A spray may be regarded as a turbulent, chemically reacting, multicomponent (MC) flow with phase change involving thermodynamics, heat and mass transport, chemical kinetics and fluid dynamics. Because of these complexities, direct studies on spray combustion may be tedious and inaccurate, hence an essential prerequisite for understanding spray phenomenon is the knowledge of the laws governing droplet evaporation and combustion.

Further, the submillimeter scales associated with spray problem have made detailed experimental measurements quite difficult. Hence in general, theory and computations have led experiments in analysing spray systems [1].

Spherically symmetric droplet combustion can be achieved experimentally through drop towers (a specially designed freely falling droplet combustion apparatus) which provides a microgravity environment by eliminating buoyancy and offers a simplified geometry of the combustion environment for analysing droplet processes in detail.

Isoda and Kumagai [2,3,4] were pioneers in conducting spherically symmetric droplet combustion experiments in drop towers capturing the flame movement and further showed that *F/D* ratio varies throughout the droplet burning history.

1.1 Quasi-steady, QS-Transient and Transient Vaporisation and Combustion of Single Droplets

In the quasi-steady approach, system is spherically symmetric, droplet is at its boiling point, d^2*-law* is followed, gas phase proceesses are occuring at a very fast rate as compared to liquid phase processes, flame to droplet diameter ratio is a large constant value, properties are assumed constant.

Waldman [5] and Ulzama and Specht [6] used analytical procedure whereas Puri and Libbi [7] and King [8] employed numerical techniques in

developing spherically symmetric droplet combustion models. The results of these authors were mainly confined to the observations that unlike quasi-steady case, flame is not stationary and flame to droplet diameter ratio increases throughout the droplet burning period.

Most of the theoretical studies considered either quasi-steady liquid phase with unsteady gas phase or vice-versa [1]. Whereas, fully transient models can be employed in multicomponent droplet vaporisation and combustion studies.

1.2 Droplet Vaporisation and Combustion in Convective Environment

Droplet combustion in convective environment can be modelled using forced convective correlations [9,1,10,11]. Ranz and Marshall correlation [12] based on heat transfer which is frequently used corresponds to a correction factor of $1+0.3Re_g^{0.5}Pr_g^{0.33}$, where gas phase Reynolds number Re_g is based on droplet diameter.

Yang and Wong [13] investigated the effect of heat conduction through the support fibre on a droplet vaporising in a weak convective field.

1.3 Effect of Ambient Parameters on Droplet Vaporisation and Combustion

Chin and Lefebvre [14] investigated the effects of ambient pressure and temperature on steady state combustion of commercial fuels like aviation gasoline, JP5 and diesel oil (DF2). Their results suggested that evaporation constant values were enhanced as ambient pressure and temperature were increased.

Kadota and Hiroyasu [15] conducted an experimental study of single suspended alkanes and light oil droplets under natural convection in supercritical gaseous environment at room temperatures. It was noted that combustion lifetime decreased steeply with an increase in reduced pressure till the critical point whereas burning constant showed a continuously increasing trend with reduced pressure in both sub and supercritical regimes.

Deplanque and Sirignano [16] developed an elaborate numerical model to investigate spherically symmetric, transient vaporisation of a liquid oxygen (LOX) droplet in supercritical gaseous hydrogen. They advocated the use of Redlich-Kwong EOS and suggested it can be assumed that dissolved hydrogen remains confined in a thin layer at the droplet surface. Further it was observed that vaporisation process followed the .

Zhu and Aggarwal [17] performed numerical investigation of supercritical vaporisation phenomena for n-heptane–N_2 system by considering transient, spherically symmetric conservation equations of both gas and liquid phases, pressure dependent properties and detailed treatment of liquid-vapour phase equilibrium employing different EOS.

Yang [18] also analysed numerically a fully transient model for LOX-H_2 system employing complex Benedict-Webb-Rubin EOS. Vieille et al.[19] conducted microgravity combustion experiments of 1.5mm diameter alkane and alcohol droplets using suspended droplet technique in high pressure air at 300K. An important result was that d^2*-law* was followed even under supercritical pressure of 120 bar.

Stengele et al.[20] conducted experimental and theoretical study of freely falling single and bicomponent (n-pentane, n-nonane) droplets in a stagnant high pressure N_2 gas at different temperatures incorporating convective effects. The results were compared with numerical results of diffusion limit model.

Marchese et al. [21] modelled spherically symmetric n-heptane droplet combustion in a (30% O_2-70% He) environment and obtained the extinction diameter which is an important aspect of droplet combustion (occuring when the flame extinguishes before the droplet is consumed).

II. Problem Formulation

2.1 Introduction

As mentioned before, droplet combustion experiments have shown that liquid droplet burning is a transient phenomenon. This is verified by the fact that the flame diameter first increases and then decreases and flame to droplet diameter ratio increases throughout the droplet burning unlike the simplified analyses where this ratio assumes a large constant value. Keeping this in mind, an unsteady, spherically symmetric, single component, diffusion controlled gas phase droplet combustion model was developed by solving the transient diffusive equations of species and energy.

2.2 Development of spherically symmetric, unsteady droplet combustion model for the gas phase

Important assumptions invoked in the development of spherically symmetric gas phase droplet combustion model of the present study

Spherical liquid fuel droplet is made up of single chemical species and is assumed to be at its boiling point temperature surrounded by a spherically symmetric flame, in a quiescent, infinite oxidising medium with phase equilibrium at the liquid-vapour interface expressed by the Clausius-Clapeyron equation.

Droplet processes are diffusion controlled (ordinary diffusion is considered, thermal and pressure diffusion effects are neglected). Fuel and oxidiser react instantaneously in stoichiometric proportions at the flame. Chemical kinetics is infinitely fast resulting in flame being represented as an infinitesimally thin sheet.

Ambient pressure is subcritical and uniform. Conduction is the only mode of heat transport, radiation heat transfer is neglected. Soret and Dufour effects are absent.

Thermo physical and transport properties are evaluated as a function of pressure, temperature and composition. Ideal gas behaviour is assumed. Enthalpy 'h' is a function of temperature only. The product of density and diffusivity is taken as constant. Gas phase Lewis number Le_g is assumed as unity.

The overall mass conservation and species conservation equations are given respectively as:

$$\frac{\partial \rho}{\partial t}+\frac{1}{r^2}\frac{\partial}{\partial r}\left(r^2 \rho v_r\right)=0 \qquad (1)$$

$$\frac{\partial(\rho Y)}{\partial t}+\frac{1}{r^2}\frac{\partial}{\partial r}r^2\left[\rho v_r Y-\rho D\frac{\partial Y}{\partial r}\right]=0 \quad (2)$$

Where;

t is the instantaneous time

r is the radial distance from the droplet center

ρ is the density

v_r is the radial velocity of the fuel vapour

D is the mass diffusivity

Y is the mass fraction of the species

equations (1) and (2) are combined to give species concentration or species diffusion equation for the gas phase as follows

$$\frac{\partial Y}{\partial t}=D_g\frac{\partial^2 Y}{\partial r^2}+\frac{2D_g}{r}\frac{\partial Y}{\partial r}-v_r\left(\frac{\partial Y}{\partial r}\right) \qquad (3)$$

D_g is the gas phase mass diffusivity

The relation for energy conservation can be written in the following form

$$\frac{\partial(\rho h)}{\partial t}+\frac{1}{r^2}\frac{\partial}{\partial r}\left[r^2\rho\left(v_r\cdot h-D.\,C_p\frac{\partial T}{\partial r}\right)\right]=0 \quad (4)$$

The energy or heat diffusion equation for the gas phase, equation (5) can be derived with the help of overall mass conservation equation (1) and equation (4), as:

$$\frac{\partial T}{\partial t}=\alpha_g\frac{\partial^2 T}{\partial r^2}+\frac{2\alpha_g}{r}\frac{\partial T}{\partial r}-v_r\left(\frac{\partial T}{\partial r}\right) \qquad (5)$$

T is the temperature, α_g is gas phase thermal diffusivity. Neglecting radial velocity of fuel vapour v_r for the present model, equations (3) and (5) reduce to a set of linear, second order partial differential equations (eqns 6 and 7).

$$\frac{\partial Y}{\partial t}=D_g\frac{\partial^2 Y}{\partial r^2}+\frac{2D_g}{r}\frac{\partial Y}{\partial r} \qquad (6)$$

$$\frac{\partial T}{\partial t}=\alpha_g\frac{\partial^2 T}{\partial r^2}+\frac{2\alpha_g}{r}\frac{\partial T}{\partial r} \qquad (7)$$

The solution of these equations provide the species concentration profiles (fuel vapour and oxidiser) and temperature profile for the inflame and post flame zones.

The boundary and initial conditions based on this combustion model are as follows

$$at\ r=r_f;\ T=T_f,\ Y_{o,f}=0,\ Y_{F,f}=0$$

$$at\ r=r_\infty;\ T=T_\infty,\ Y_{o,\infty}=0.232,$$

$$at\ t=0;\ r=r_{lo},\ T=T_b,\ Y_{F,S}=1.0$$

$$\text{where}\quad r_l=r_{lo}\left(1-t/t_d\right)^{1/2}\quad \text{for}\quad \left(0\le t\le t_d\right),$$

is the moving boundary condition coming out from the d^2-*law* (since droplet is at its boiling point temperature). Here, T_f and T_∞ are temperatures at the flame and ambient atmosphere respectively. $Y_{F,S}$ and $Y_{F,f}$ are fuel mass fractions respectively at the droplet surface and flame. $Y_{o,\infty}$ and $Y_{o,f}$ are oxidiser concentrations in the ambience and at the flame respectively, t is the instantaneous time, t_d is the combustion lifetime of the droplet, r_{lo} is the original or initial droplet radius and r_l is the instantaneous droplet radius at time "t".

The location where the maximum temperature $T=T_f$ or the corresponding concentrations $Y_{F,f}=0$ and $Y_{o,f}=0$ occur, was taken as the flame radius r_f. Instantaneous time "t" was obtained from the computer results whereas the combustion lifetime "t_d" was determined from the relationship coming out from the d^2-*law*. Other parameters like instantaneous flame to droplet diameter ratio (F/D), flame standoff distance $(F\text{-}D)/2$, dimensionless flame diameter (F/D_0) etc, were then calculated as a function of time

Solution technique

Equations (6) and (7) were solved numerically using the "finite difference technique". The approach is simple, fairly accurate and numerically efficient [22]. Here the mesh size in radial direction was chosen as h and in time direction as k. Using finite difference approximations, equations (6) and (7) were descritised employing three point central difference expressions for second and first space derivatives, and the time derivative was approximated by a forward

difference approximation resulting in a two level, explicit scheme (equation 8) which was implemented on a computer.

$$T_m^{n+1} = \alpha\lambda_1\left(1-p_m\right)T_{m-1}^n + \left(1-2\alpha\lambda_1\right)T_m^n + \alpha\lambda_1\left(1+p_m\right)T_{m+1}^n \qquad (8)$$

Here, $\lambda_1(mesh\ ratio) = k/h^2$, $p_m = h/r_m$, $r_m = r_{lo} + mh$, $Nh = r_\infty - r_{lo}$, $m = 0,1,2....N$.

The solution scheme is stable as long as the stability condition $\lambda_1 < 1/2$ is satisfied.

2.3 Estimation of flame temperature

In the present work, thermodynamic and transport properties were evaluated on the basis of flame temperature and ambient temperature for the outer or the post flame zone and boiling point temperature and flame temperature for the inner or inflame zone. Accuracy of the evaluated properties depend upon the correct estimation of flame temperature and play a vital role in predicting combustion parameters and their comparison with the experimental results. A computer code was developed in the present work for determining the adiabatic flame temperature using first law of thermodynamics with no dissociation effects.

A more accurate method like Gülder [23] (described below) which incorporates dissociation, multicomponent fuels and high temperature and pressure effects was also used for getting flame temperature. An expression of the following form has been adopted to predict the flame temperature, which is applicable for the given ranges:

$$[0.3 \le \phi \le 1.6;\ 0.1MPa \le P \le 7.5MPa;\ 275K \le Tu \le 950K;\ 0.8 \le H/C \le 2.5]$$

$$T_{adiabatic} = A\sigma^\alpha.\exp\left[\beta\left(\sigma+\lambda\right)^2\right].\pi^x\theta^y\psi^z \qquad (9)$$

where,

$x = a_1 + b_1\sigma + c_1\sigma^2$

$y = a_2 + b_2\sigma + c_2\sigma^2$

$z = a_3 + b_3\sigma + c_3\sigma^2$

π is dimensionless pressure = P/P_o (P_o = 0.1013 MPa)

θ is dimensionless initial mixture temperature $= T_u/T_a$

T_a = 300 K

ψ is H/C atomic ratio

σ = ϕ for $\phi \le 1$ (ϕ is the fuel-air equivalence ratio defined as $(F/A)_{actual}/(F/A)_{stoichiometric}$) and

σ = $\phi - 0.7$, for $\phi > 1$

Now, $T_u = \dfrac{C_{pf}T_l + \left(A/F\right)C_{pa}T_a - L}{C_{pf} + \left(A/F\right)C_{pa}}$ (10)

C_{pf} is the specific heat of fuel vapour

C_{pa} is the specific heat of air obtained from standard air tables

T_l is the liquid fuel temperature

C_{pf} = (0.363 + 0.000467.T_b)(5 - 0.001 ρ_{fo}) (kJ/kgK)

ρ_{fo} is density of fuel at 288.6 K

T_b is boiling point Temperature (K)

$\psi = 0.9479\left[T_{mb}/100\right]^{0.2527}\cdot\left[\rho_f\right]^{-2.4063}$

T_{mb} is the fuel mid boiling point (K)

ρ_f is the relative liquid density of fuel at 20 $^\circ C$

$L = (360 - 0.39T_l)/\rho_f \quad (kJ/kg)$ (11)

(latent heat of vaporization L can also be evaluated from Reid et al. [24])

Once ϕ and θ are known, Table 1, [23] can be consulted for choosing constants $A, \alpha, \beta, \lambda, a_1, b_1, c_1, a_2, b_2, c_2, a_3, b_3, c_3$ to be used in equation (11).

After determining the flame temperature, the reference temperatures for the inflame and post flame zones respectively can be calculated using average values given as:

$T_{ref1} = (T_b + T_f)/2$ and $T_{ref2} = (T_f + T_\infty)/2$ (12)

or by using 1/3 rule [30], given as:

$T_{ref1} = (1/3)T_b + (2/3)T_f$ and

$T_{ref2} = (1/3)T_f + (2/3)T_\infty$ (13)

For the present gas phase model, thermodynamic and transport properties like specific heats, diffusion coefficients, thermal conductivities, latent heats, densities, were evaluated as a function of reference temperature and pressure from different correlations along with proper mixing rules [24]. Combustion parameters like heat transfer number B_T, burning constant k_b, combustion lifetime of the droplet t_d and mass burning rate m_f were then calculated on the basis of these properties from the following correlations.

$$B_T = \frac{\dfrac{\Delta h_c}{\nu} + C_{pg}\left(T_\infty - T_b\right)}{L} \qquad (14)$$

$$k_b \equiv -\frac{d}{dt}\left(D^2\right) = \frac{8\lambda_g}{C_{pg}\rho_l}\ln\left[1+B_T\right] \qquad (15)$$

$$t_d = D_0^{\,2}/k_b \qquad (16)$$

$$m_f = \frac{\pi r_l \rho_l k_b}{2} \qquad (17)$$

where, $\nu \rightarrow$ $(A/F)_{stoich}$ on mass basis, $\Delta h_c \rightarrow$ heat of combustion of fuel, $D_0, D \rightarrow$ original and instantaneous droplet diameters respectively, $\lambda_g \rightarrow$ thermal conductivity of the gas, $C_{pg} \rightarrow$ specific heat of the gas, $\rho_l \rightarrow$ liquid density,

2.4 Chemical Equilibrium Composition

The Olikara and Borman model [25] considered combustion reaction between fuel $C_nH_mO_lN_k$ and air at variable fuel-air equivalence ratio ϕ, temperature T and pressure P. Following equation was considered for representing combustion reaction between fuel and air:

$$x_{13}\left[C_nH_mO_lN_k + \frac{n+m/4-l/2}{\phi}\left\{O_2+3.7274N_2+0.0444Ar\right\}\right] \rightarrow x_1H + x_2O + x_3N + x_4H_2 + x_5OH + x_6CO + x_7NO + x_8O_2 + x_9H_2O + x_{10}CO_2 + x_{11}N_2 + x_{12}Ar \qquad (18)$$

Where x_1 through x_{12} are mole fractions of the product species and n, m, l and k are the atoms of carbon, hydrogen, oxygen and nitrogen respectively in the fuel. The number n and m should be non-zero while l and k may or may not be zero.

The number x_{13}, represents the moles of fuel that will give one mole of products. In addition to carbon and hydrogen, the fuel may or may not contain oxygen and nitrogen atoms. In the present study, fuels considered were free from nitrogen atoms. The product species considered were $H, O, N, H_2, OH, CO, NO, O_2, H_2O, CO_2$, N_2 and Ar in gas phase [25]. Whereas in the present work, only CO, NO, CO_2 and H_2O were considered for the sake of simplicity.

The equilibrium constants used in the programme [25] were fitted as a function of temperature in the range $(600K - 4000K)$. It was shown that equivalence ratio,

$$\phi = \frac{AN + 0.25AM - 0.5AL}{0.5AN - 0.5AL} \qquad (19)$$

(where AN, AM, AL are the number of C, H and O atoms in fuel molecules). The products of combustion were assumed to be ideal gases (assumption not valid at extremely high pressures). The gas phase code developed in the present work was used with the Olikara and Borman code [25] for calculating the equilibrium composition of combustion products representing species concentration profiles around a burning droplet. Important steps of this programme and detailed kinetic mechanism are given in [25].

III. Results and Discussion

3.1 Effect of Ambient Temperature on Adiabatic Flame Temperature and Burning Constant

Figure 1 shows the variation of adiabatic flame temperature T_f (calculated using Gülder's method) [23] with ambient temperature T_∞ ranging from $298\,K$ to $1500\,K$ for a $2000\,\mu m$ n-heptane droplet combusting at ambient pressure $P_\infty = 1$ atmosphere and ambient oxidiser concentration $Y_{o,\infty} = 0.232$. From Figure 2, it is observed that burning constant is increasing gradually with an increase in ambient temperature. The reason is mainly due to an increase in the value of adiabatic flame temperature with ambient temperature T_∞. Since thermophysical properties were estimated on the basis of the flame temperature, they further influence the combustion parameters like k_b, t_d and m_f.

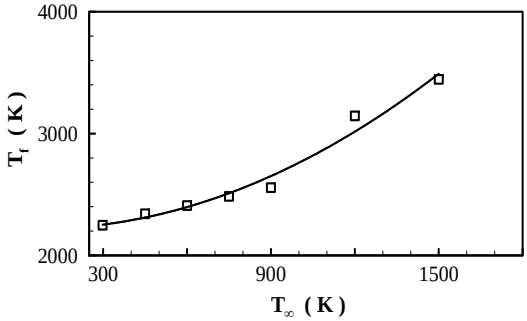

Figure 1: Effect of ambient temperature on adiabatic flame temperature

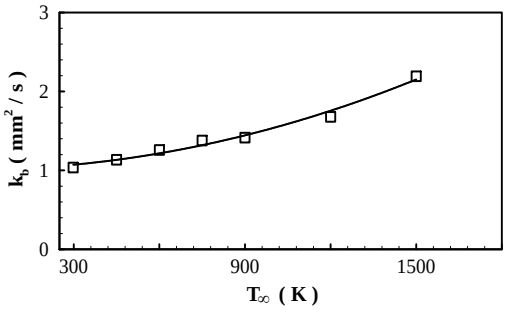

Figure 2 : Burning constant

3.2 Droplet Lifetime and Mass Burning Rate

Figure 3 shows the variation of ambient temperature on the combustion lifetime for a 1000 μm n-heptane droplet. It is seen that values of combustion lifetime predicted by the present model decrease with an increase in the ambient temperature. This behaviour is true because the droplet lifetime t_d is inversely proportional to k_b from the relationship coming out of the $d^2 - law$.

From Figure 4 it is observed that mass burning rate m_f increases with an increase in ambient temperature T_∞, which was varied from 298 K to 1500 K. The burning rate was obtained from equation 17. For a fixed droplet radius, the burning rate is found to be a strong function of burning constant k_b and thus m_f increases with the increase in ambient temperature.

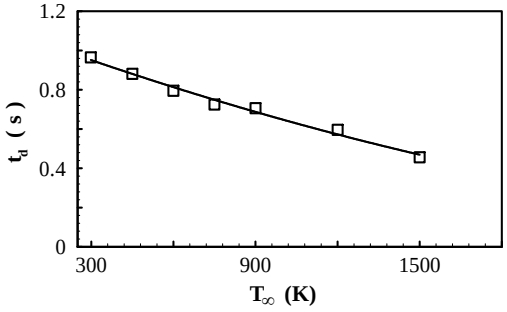

Figure 3 : Droplet lifetime

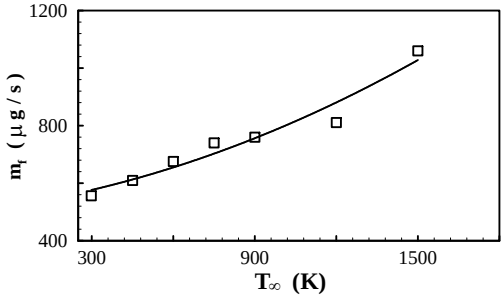

Figure 4: Droplet mass burning rate

3.3 Temperature Effect on Emission Characteristics of a Spherically Symmetric n-Heptane Burning Droplet

It is observed from Figure 5 for a 100 μm n-heptane droplet burning in standard atmosphere, that as ambient temperature is increased from 298 K to 900 K, the corresponding NO concentration is also increased. As stated earlier, NO concentrations are strongly dependent upon flame temperature and are found to increase appreciably with increase in flame temperature. However, these results are aimed at providing a general qualitative trend only. Refer Table 2.

It is further observed that as ambient temperature is increased, then due to a corresponding increase in the flame temperature, dissociation of CO_2 increases, hence rate of CO formation is increased with increase in ambient temperature (Figure 7). On the contrary, the rate of formation of CO_2 (Figure 6), decreases with an increase in the ambient temperature. Dissociation effect also decreases the H_2O concentration with an increase in T_∞ (Figure 8). The above observations for the present study are consistent with Le Chatelier principle which states that any system initially in a state of equilibrium when subjected to a change (increase in temperature or pressure) will shift in composition in such a way as to minimise the change [11].

When temperature is increased, the composition shifts in the endothermic direction. Since heat is absorbed when CO_2 breaks down into CO and O_2 hence producing a shift to the right, in the reaction: CO2 $\Leftrightarrow$ CO+1/2 O_2. The same can be said about H_2O concentration.

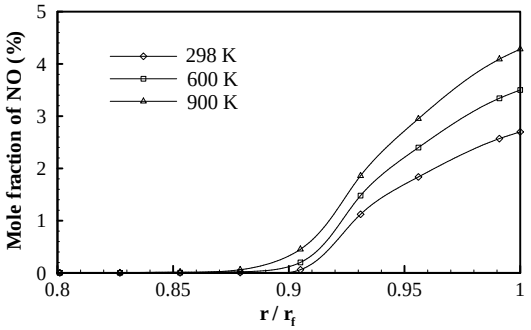

Figure 5: NO concentration variation with dimensionless flame radius at different ambient temperatures for n-heptane

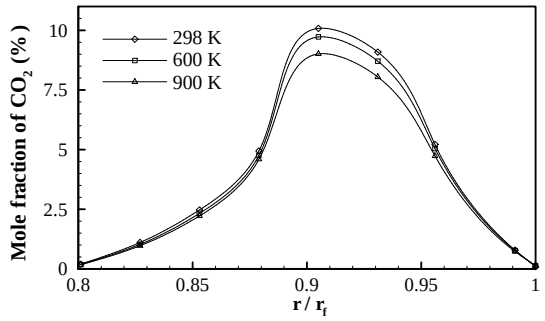

Figure 6: CO_2 concentration

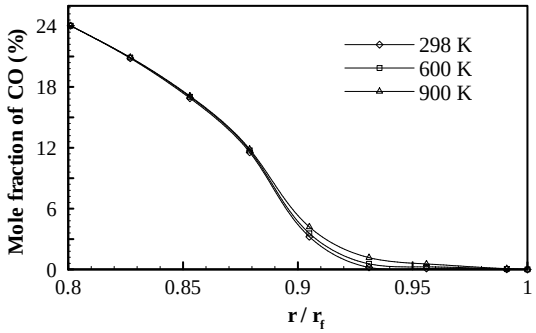

Figure 7: CO concentration

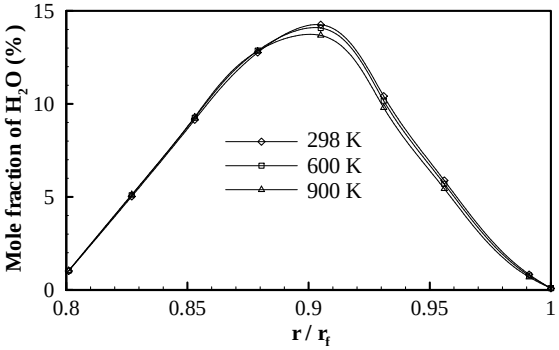

Figure 8: H_2O concentration

3.4 Effect of Variation of Ambient Oxidiser Concentration on Burning Constant k_b for Ethanol

For the present work, it is seen that as ambient oxidiser concentration is increased, adiabatic flame temperature T_f for a 2000 μm n-heptane droplet is also increased (Figure 9), Table 3. Thermophysical and transport properties were then calculated as a function of this temperature using property relations [24]. The combustion properties were evaluated next which include B_T, k_b, t_d, m_f (Table 4), using equations 14-17. The effect of these properties resulted in increased values of k_b and m_f and hence smaller burning times. The same trend of T_f increasing with T_∞ was also true for ethanol. The variation of burning constant k_b with ambient oxidiser concentration $Y_{o,\infty}$ for ethanol is depicted in Figure 10 and compared with the results of Choi et al. [26] who considered microgravity droplet combustion in varying oxygen environment. It was observed that results of present study are close to those of Choi et al, verifying the simplicity and accuracy of the gas phase model of the present work.

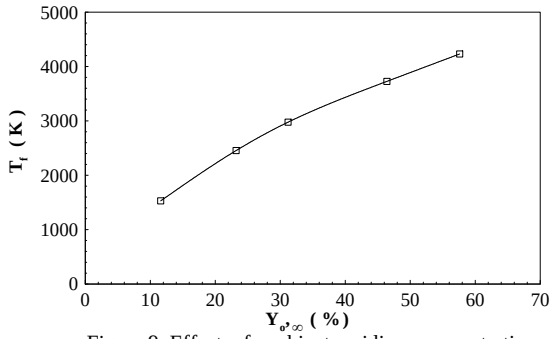

Figure 9: Effect of ambient oxidiser concentration on flame temperature

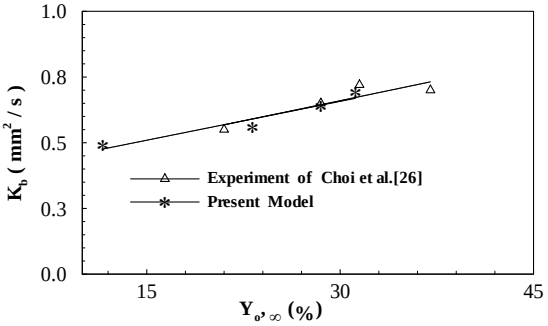

Figure 10: Effect of ambient oxidiser concentration on burning constant for ethanol (D_0 = 1800 microns, P_∞ = 1 atm, T_∞ = 298 K)

3.5 Effect of Ambient Oxidiser Concentration on T_f, k_b, t_d and m_f for n-Heptane

The variation of burning constant k_b, combustion lifetime t_d and burning rate m_f repectively as a function of ambient oxidiser concentration $Y_{o,\infty}$ for a 2000 micron n-heptane droplet burning in standard atmosphere are depicted in Figs 11-13.

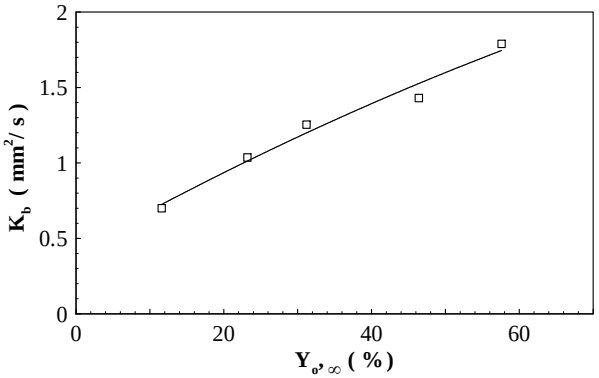

Figure 11: Burning constant

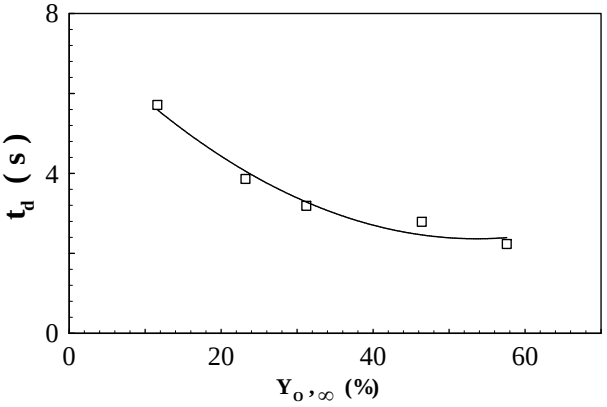

Figure 12 : Droplet lifetime

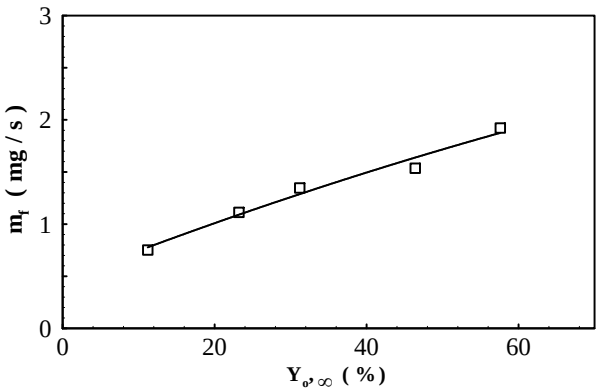

Figure 13 : Mass burning rate

3.6 Combustion Aspects of Fuel Droplet in Oxygen-Helium Atmosphere

An important aspect of spherically symmetric droplet combustion is the calculation of extinction diameter which results when the flame extinguishes before the droplet is consumed. This aspect can be controlled by mixing ambient oxygen with an inert gas such as helium which has high thermal conductivity. In this situation, gas phase chemical reactions can go to completion and extinction diameter is greatly reduced and becomes too small to measure [21,27].

Another advantage of using an inert gas is to curb the sooting tendency of the hydrocarbon fuel, such as n-heptane. In experiments with sooting fuels it is difficult to measure the extinction diameters because of the sooting effect.

For the present work, the adiabatic flame temperature was calculated as $1205\,K$ from first law of thermodynamics for stoichiometric reaction between n-heptane and (30 % O_2 + 70 % Helium). Properties of helium were taken from Gordon and McBride [28]. Combustion parameters were then determined subsequently. A comparison was obtained in the form of D^2 versus t, (Figure 14).

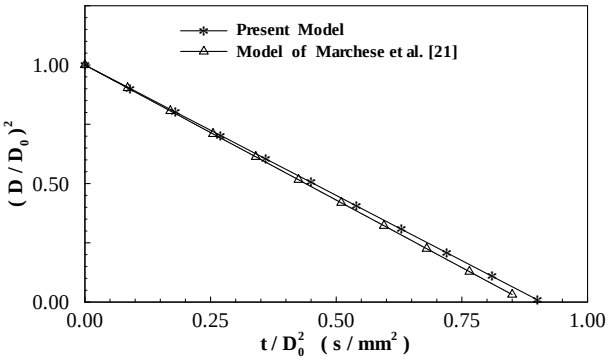

Figure 14: Variation of $(D / D_0)^2$ with t / D_0^2 for n-heptane droplet burning in 30 % O_2 / 70 % He atmosphere ; (D_0 = 3000 microns, P_∞ = 1 atm, T_∞ = 298 K)

Both scales were non-dimensionalised by D_0^2. Result of the present model was compared that of Marchese et al. [20]. O_2 and He were present as a mixture of 30 % O_2 and 70 % Helium for both models. On comparison it was observed that for both results, extinction diameters occured at times close to each other. For the present model, extinction diameter was calculated as 0.0571mm occurring at 8.253s (t / D_0^2 = 0.917s). For Marchese et al. model, the value of extinction diameter was zero at t / D_0^2 = 0.875. The small difference could be due to the determination of properties which subsequently effect the combustion parameters.

3.7 Effect of Ambient Temperature and oxidiser concentration on droplet lifetime and mass burning rate of n-heptane as a function of original droplet diameter

It was observed that at a fixed droplet diameter, an increase in temperature led to a decrease in droplet lifetime and an increase in burning rate. Whereas, both lifetime and burning rate increased with droplet size at a given temperature (Figs 15-16).

Further, for a fixed droplet size, an increase in oxidiser concentration decreased droplet lifetime and enhanced burning rate and at a particular concentration, both of these parameters increased with droplet size (Figs 17-18).

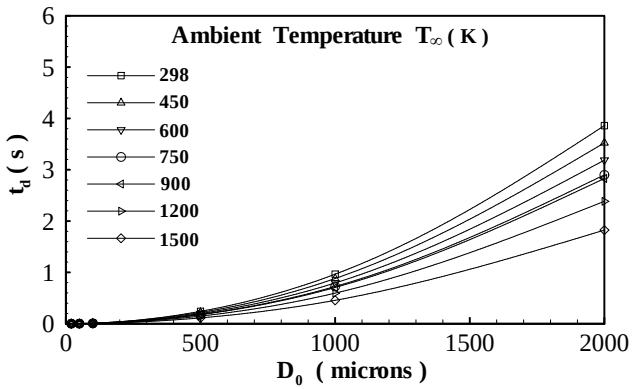

Figure 15: Initial droplet diameter effect on lifetime

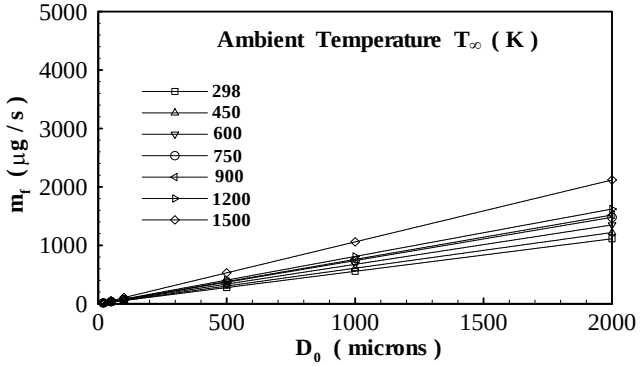

Figure 16: Droplet mass burning rate

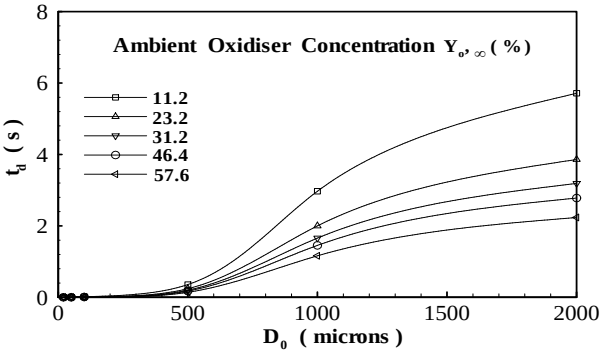

Figure 17 : Initial droplet diameter effect on droplet lifetime

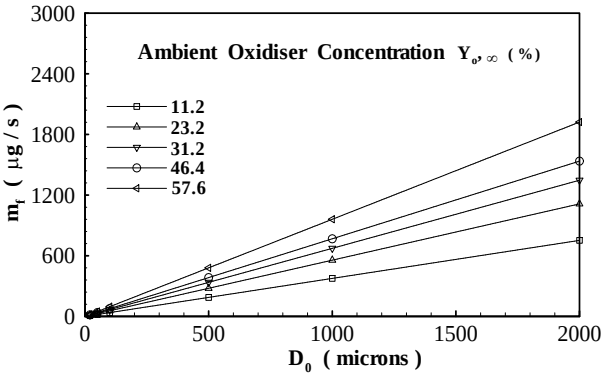

Figure 18: Droplet mass burning rate

IV. Conclusions

The effect of ambient temperature and composition on droplet burning is profound as combustion chamber temperatures in various combustion devices can exceed $2500\,K$. In the present work, for an increase in temperature from $298\,K$ to $1500\,K$, it was observed that flame temperature, burning constant and mass burning rate increased while droplet lifetime decreased for a n-heptane droplet burning in standard atmosphere. Regarding emission behaviour, it was observed that as temperature was increased from $298\,K$ to $900\,K$, NO and CO concentrations increased while CO_2 and H_2O concentrations were lowered.

Effect of increasing ambient oxidiser concentration resulted in an increase in flame temperature, burning constant and mass burning rate and a decrease in droplet lifetime for a n-heptane droplet. On comparing burning constant versus ambient oxidiser concentration behaviour for ethanol droplet of the present model with the experimental work of Choi et al. [26], it was observed that the two results were in good agreement (Figure 10). Extinction diameter obtained by the present model for a n-heptane droplet burning in oxygen-helium environment, and by Marchese et al.[21] also agreed quite well (Figure 14). A small difference could be attributed to the difference in properties. The gas phase model of the present work is accurate and yet simple for its implementation in spray combustion codes where CPU economy plays a vital role.

References

[1] W. A. Sirignano, "Fluid Dynamics and Transport of Droplets and Sprays", Cambridge University Press, 1999.

[2] S. Okajima, S. Kumagai, "Further Investigation of Combustion of Free Droplets in a Freely Falling Chamber Including Moving Droplets", Proceedings of the Fifteenth Symposium (International) on Combustion, The Combustion Institute, pp. 401-407, 1974.

[3] S. Kumagai, H. Isoda, "Combustion of Fuel Droplets in a Falling Chamber", Proceedings of the Sixth Symposium (International) on Combustion, Reinhold, N.Y., pp. 726-731, 1957.

[4] H. Isoda, S. Kumagai, "New Aspects of Droplet Combustion", Proceedings of the Seventh Symposium (International) on Combustion, The Combustion Institute, pp. 523-531, 1959.

[5] C. H. Waldman, "Theory of Non-Steady State Droplet Combustion", Fifteenth Symposium (International) on Combustion, The Combustion Institute, pp. 429-442, 1974.

[6] S. Ulzama, E. Specht, "An Analytical Study of Droplet Combustion Under Microgravity: Quasi-Steady Transient Approach", Proceedings of the Thirty First Symposium (International) on Combustion, The Combustion Institute, pp. 2301-2308, 2007.

[7] I. K. Puri, P. A. Libby, "The Influence of Transport Properties on Droplet Burning", Combustion Science and Technology, Vol. 76, pp. 67-80, 1991.

[8] M. K. King, "An Unsteady-State Analysis of Porous Sphere and Droplet Fuel Combustion Under Microgravity Conditions", Proceedings of the Twenty Sixth Symposium (International) on Combustion, The Combustion Institute, pp.1227-1234, 1996.

[9] G. M. Faeth, "Current Status of Droplet and Liquid Combustion", Progress in Energy and Combustion Science, Vol. 3, pp. 191-224, 1977.
[10] A. H. Lefebvre, "Atomization and Sprays", Hemisphere Publishing Corporation, Philadelphia, London, 1989.
[11] S. R. Turns, "An Introduction to Combustion Concepts and Applications", McGraw Hill International Edition, 1996.
[12] W. E. Ranz, W. R. Marshall, "Evaporation from Drops", Chem. Eng. Progr. 48, pp.141-146 and 173-180, 1952.
[13] J. Yang, S. Wong, "On the Discrepancies Between Theoretical and Experimental Results for Microgravity Droplet Combustion", Int. J. Heat Mass Transfer, Vol. 44, pp. 4433-4443, 2001.
[14] J. S. Chin, A. H. Lefebvre, "Steady-State Evaporation Characteristics of Hydrocarbon Fuel Drops", AIAA Journal, Vol. 21, No.10, pp.1437-1443, 1983.
[15] T. Kadota, H. Hiroyasu, "Combustion of a Fuel Droplet in Supercritical Gaseous Environments", Proceedings of the Eighteenth Symposium (International) on Combustion, The Combustion Institute, pp. 275-282, 1981.
[16] J. P. Delplanque, W. A. Sirignano, "Numerical Study of the Transient Vaporization of an Oxygen Droplet at Sub and Supercritical Conditions" Int. J. Heat Mass Transfer, Vol. 36, pp. 303-314, 1993.
[17] G. Zhu, S. K. Aggarwal, "Transient Supercritical Droplet Evaporation with Emphasis on the Effects of Equation of State", Int. J. Heat Mass Transfer, Vol. 43, pp. 1157-1171, 2000.
[18] V. Yang, "Modelling of Supercritical Vaporization, Mixing and Combustion Processes in Liquid Fueled Propulsion Systems", Proceedings of the Twenty Eighth Symposium (International) on Combustion, The Combustion Institute, pp. 925-942, 2000.
[19] Vieille et al, "High Pressure Droplet Burning Experiments in Microgravity", Proceedings of the Twenty Sixth Symposium (International) on Combustion, The Combustion Institute, pp. 1259-1265, 1996.
[20] J. Stengele, K. Prommersberger, M. Willmann, S. Wittig, "Experimental and Theoretical Study of One and Two Component Droplet Vaporization in a High Pressure Environment", Int. J. Heat Mass Transfer, Vol. 42, pp. 2683-2694, 1999.
[21] A. J. Marchese, F. L. Dryer, V. Nayagam, "Numerical Modeling of Isolated n-Alkane Droplet Flames: Initial Comparisons with Ground and Space-Based Microgravity Experiments", Combustion and Flame, Vol.116, pp. 432- 459, 1999.
[22] M. K. Jain, "Numerical Solution of Differential Equations", Second Edition, Wiley-Eastern Limited, 1984.
[23] Ö. L. Gülder, "Flame Temperature Estimation of Conventional and Future Jet Fuels", Transactions of the ASME, Vol. 108, pp. 376-380, 1986.
[24] R. C. Reid, J. M. Prausnitz, B. E. Poling, "The Properties of Gases and Liquids", Fourth Edition, McGraw Hill Book Company, 1989.
[25] C. Olikara, G. L. Borman, "A Computer Program for Calculating Properties of Equilibrium Combustion Products with some Application to I.C. Engines", SAE Paper 750468, SAE Trans, 1975.
[26] Choi et al, "Ethanol Droplet Combustion at Elevated Pressures and Enhanced Oxygen Concentrations", AIAA, 41st Aerospace Sciences Meeting and Exhibit, Reno, Nevada, pp. 1-7, 2003.
[27] Nayagam et al, "Microgravity n-Heptane Droplet Combustion in Oxygen-Helium Mixtures at Atmospheric Pressures", AIAA Journal, Vol. 36, No. 8, 1998.
[28] S. Gordon, B. J. McBride, "Thermodynamic Data to 20000 K for Monatomic Gases", NASA/TP−1999-208523, June 1999.

Table 1: Constants for Evaluating Flame Temperature by Gülder's Method [23]

Constants	$0.3 \le \phi \le 1.0$		$1.0 < \phi \le 1.6$	
	$0.92 \le \theta < 2$	$2 \le \theta \le 3.2$	$0.92 \le \theta < 2$	$2 \le \theta \le 3.2$
A	2361.7644	2315.7520	916.8261	1246.1778
α	0.1157	-0.0493	0.2885	0.3819
β	-0.9489	-1.1141	0.1456	0.3479
λ	-1.0976	-1.1807	-3.2771	-2.0365
a_1	0.0143	0.0106	0.0311	0.0361
b_1	-0.0553	-0.0450	-0.0780	-0.0850
c_1	0.0526	0.0482	0.0497	0.0517
a_2	0.3955	0.5688	0.0254	0.0097
b_2	-0.4417	-0.5500	0.2602	0.5020
c_2	0.1410	0.1319	-0.1318	-0.2471
a_3	0.0052	0.0108	0.0042	0.0170
b_3	-0.1289	-0.1291	-0.1781	-0.1894
c_3	0.0827	0.0848	0.0980	0.1037

Table 2: Variation of NO,CO, CO_2 and H_2O Concentrations with Ambient Temperature for n-Heptane

Ambient temperature (K)	**Adiabatic flame temperature (K)**	**NO (%)**	**CO (%)**	**CO_2 (%)**	**H_2O (%)**
298	2247.67	2.6984	3.2389	10.082	14.255
600	2409.44	3.5004	3.5628	9.7232	14.089
900	2556.30	4.2816	4.1981	9.0127	13.681

Table 3: Variation of Adiabatic Flame Temperature with Ambient Oxidiser Concentration for n-Heptane

Oxidiser concentration (%) $Y_{o,\infty}$	**Adiabatic flame temperature (K)** T_f
11.2	1528.57
23.2	2247.67
31.2	2976.9
46.4	3726.68
57.6	4230.72

Table 4: Effect of $Y_{o,\infty}$ on B_T, k_b, t_d and m_f for n-Heptane ($D_0 = 2000\mu m$)

Ambient oxidiser concentration $Y_{o,\infty}(\%)$	**Heat transfer No** B_T	**Burning constant** $k_b(mm^2/s)$	**Droplet lifetime** $t_d(s)$	**Mass burning rate** $m_f\ (mg/s)$
11.2	4.17	0.7	5.714	0.752
23.2	8.765	1.036	3.86	1.113
31.2	11.85	1.254	3.1897	1.347
46.4	17.86	1.43	2.78	1.536
57.6	22.27	1.789	2.235	1.922